

Accelerator Deflection-Mode Dampening Experiments at Argonne

E. Chojnacki, W. Gai, C. Ho, R. Konecny, S. Mtingwa,
J. Norem, M. Rosing, P. Schoessow, and J. Simpson
Argonne National Laboratory, Argonne, IL, 60439, USA

Introduction

As the dimensions of accelerating structures become smaller and beam intensities higher, the non-axisymmetric wake fields driven by the beam become quite large even with slight misalignments of the beam from the geometrical axis. These deflection modes then cause bunch-to-bunch beam breakup and intra-bunch head-tail instabilities. An rf slow-wave structure that has very low Q for the deflection modes while maintaining a high Q for the accelerating modes would then be desirable since the unwanted modes can be selectively damped.[1] Such a device utilizing dielectric-lined waveguide is shown in Fig. 1 where the uniform outer conductor is replaced by axial, closely spaced, insulated wires which allow only axial wall currents to flow at that boundary. This dielectric-based configuration is of specific interest to the Čerenkov wake-field accelerator program under development at Argonne.[2] A configuration consistent with traditional iris-loaded waveguide is shown in Fig. 2 where the outer conductor is segmented to allow only axial currents and the irises are segmented to allow only radial currents. Severe enough damping in either configuration to eliminate the head-tail instability could be difficult to obtain depending on the bunch length considered, but strong enough damping to combat bunch-to-bunch beam breakup using these schemes appears quite feasible. Presented here will be experimental results of the dielectric-lined waveguide case.

Mode Considerations

The desired accelerating modes in slow-wave structures are TM_{01} in nature, consisting of many axial harmonics in iris-loaded waveguide or consisting of one pure mode in dielectric-lined waveguide. These axisymmetric TM_{0n} modes exert negligible deflecting force on a relativistic particle, the force having amplitude proportional to $1/\gamma^2$, where γ is the relativistic mass factor of the particle. Deflection modes are non-axisymmetric hybrids containing both axial electric and magnetic fields. The hybrid modes are labeled HEM_{mn} where m refers to the azimuthal harmonic and n is an ordering index not necessarily referring to radial harmonics. At cutoff, the dispersion relation for these hybrids degenerates to the conventional TM_{mn} and TE_{mn} waveguide modes, although the field amplitudes for TE modes are identically zero at cutoff. Of interest here, deflection modes for dielectric-lined waveguide, are the HEM_{11} , HEM_{21} , and HEM_{12} modes which correspond to the TE_{11} , TE_{21} , and TM_{11} modes at cutoff, respectively.

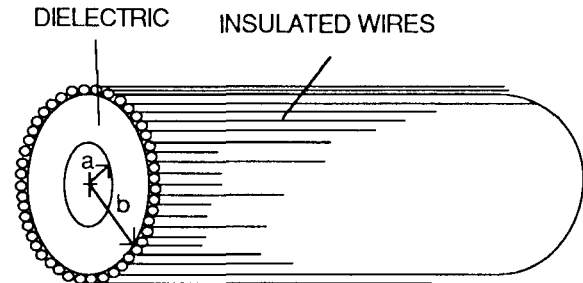


Figure 1: Dielectric-lined waveguide with segmented outer conductor.

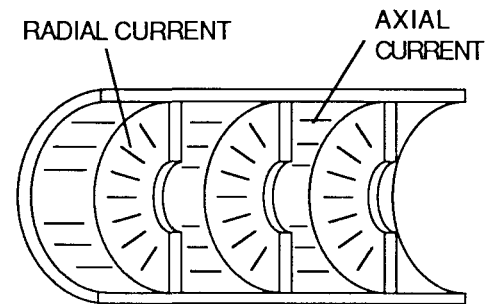


Figure 2: Iris-loaded waveguide with segmented outer conductor and segmented irises.

The rf field components of TM_{0n} modes are E_r , B_θ , and E_z . The surface currents on an outer conducting boundary necessary to support these modes are strictly axial and surface currents on irises, if any, are strictly radial. The segmented conductors on the waveguides shown in Figs. 1 and 2 will then contain these modes unperturbed, just as though the conductors were uniform.

The non-axisymmetric deflection modes, however, are comprised of all six cylindrical field components and will require azimuthal surface currents on various regions of the conductors in addition to axial and radial surface currents. If the conductors are segmented to allow only axial surface currents, the deflection modes will not be confined and will radiate beyond the outer wall, establishing a surface wave or trapped mode within a subsequent uniformly conducting boundary (vacuum vessel). This outer region can then be filled with rf absorbing material and the deflecting modes will be severely attenuated.

Bench Measurements

All bench measurements and direct wake-field measurements were performed on dielectric-lined waveguide with

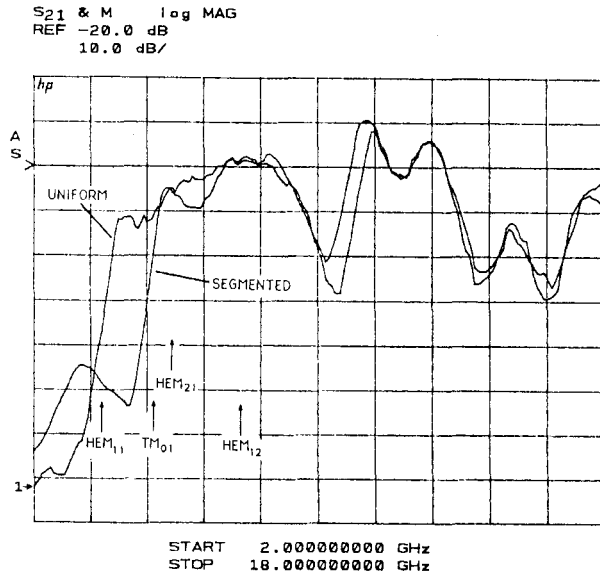


Figure 3: Network analyzer transmission measurements of dielectric-lined waveguide with and without segmented outer conductor.

dimensions $a = 1.270$ cm, $b = 1.905$ cm, and relative permittivity $\epsilon_r = 2.55$. The modes and frequencies of interest are listed in Table I. As illustrated in Fig. 1, the segmented outer conductor consisted of 173 epoxy-insulated #21 copper magnet wires strung axially in intimate contact. The parameter measured with the network analyzer was transmission coefficient S_{21} using small coupling loops at each end of a 17 cm long sample waveguide. Shown in Fig. 3 are S_{21} measurements as a function of frequency for the two cases of dielectric-lined waveguide with uniform outer conductor and with segmented outer conductor wrapped with rf absorber. The measurements should be viewed relative to each other due to coupling probe mismatches. Various mode cutoffs are indicated on the figure and the attenuation of the HEM_{11} mode is obvious. The attenuation of the HEM_{21} and HEM_{12} modes is obscured, however, by the propagation of the TM_{01} mode above cutoff.

Table I. Mode cutoffs and frequencies synchronous with a 20 MeV electron for dielectric-lined waveguide having $a = 1.27$ cm, $b = 1.905$ cm, and $\epsilon_r = 2.55$.

Mode	Cutoff (GHz)	Synchronous (GHz)
HEM_{11}	3.96	6.76
TM_{01}	5.44	7.64
HEM_{21}	5.85	8.40
HEM_{12}	7.82	12.18

From the measurements shown in Fig. 3, which again, are relative to probe coupling mismatches, the damped HEM_{11} mode has an additional attenuation of $\alpha_{dB} \sim 235$ dB/m above that of normal resistive wall losses. Ignoring resistive wall losses, the attenuation e-folding time and cavity Q for this mode can then be found from

$$\tau = \frac{1}{\alpha_t} = \frac{8.686}{\alpha_{dB} v_g} \quad \text{and} \quad (1)$$

$$Q = \frac{\omega}{2\alpha_t v_g}, \quad (2)$$

where α_t is the attenuation in units of [nepers/sec], α_{dB} is the attenuation in units of [dB/m], v_g is the group velocity of the particular mode, 8.686 is a dB-neper conversion factor, and ω is the angular frequency of the mode. For all of the modes in question, $v_g \sim c/2$ to within 10%, thus for the HEM_{11} mode $\tau \sim 246$ ps and $Q \sim 5.2$.

Direct Wake-Field Measurements

Direct measurements of beam induced wake fields in the above described dielectric-lined waveguide were performed at the Advanced Accelerator Test Facility (AATF) at Argonne.[3] In this facility a 20 MeV, 30 ps, 5 nC drive bunch excites wake fields in any test structure and the fields are then sampled by a much less intense 15 MeV witness bunch which has a variable-delay behind the drive bunch. The wake fields are quantified by viewing the witness in an energy spectrometer.

The two dielectric-lined waveguide structures tested had parameters as listed in Table I and were 52 cm in length. One had a uniform aluminum outer conductor while the other had the segmented conductor described previously. Shown in Fig. 4 are the measured *longitudinal* wake functions for the two structures normalized to 1 m of axial length and 1 nC of drive charge. The enhanced wake amplitude during the first cycle, $\lesssim 120$ ps, is due to several higher order TM_{0n} modes being nearly in phase at that time. The slow, linear decrease of longitudinal wake thereafter is due to rf power exiting the interaction region at the mode's group velocity. Shown in Fig. 5 are the Fourier transforms of the longitudinal wakes and the principle mode seen for both structures is the TM_{01} , agreeing with the calculated frequency of 7.64 GHz. Within measurement uncertainty there is negligible difference between the two structures in longitudinal wake amplitude or frequency.

The deflection modes have field amplitudes proportional to $I_m(\omega r_0/c\beta\gamma)$, where I_m is the modified Bessel function, ω is the mode's angular frequency, r_0 is the drive bunch radial coordinate, c is the speed of light, $\beta\gamma$ are normalized velocity and relativistic mass factor associated with the wave phase velocity, and $m \geq 1$ is the mode's azimuthal harmonic. In the limit of phase velocity approaching the speed of light, the argument of I_m approaches zero and the deflection modes then have field amplitudes proportional to r_0^m . The fields seen by the witness, however, have functional dependence on witness radial position given by r^{m-1} . The deflecting force on the witness bunch is then proportional to $r_0^m r^{m-1}$ and for dipole modes ($m = 1$) this is simply linearly proportional to the drive bunch radial position. Thus, the transverse wake function for the dominant deflection mode (dipole) can be determined by measuring the transverse deflection of the witness for several drive bunch radial positions, checking for

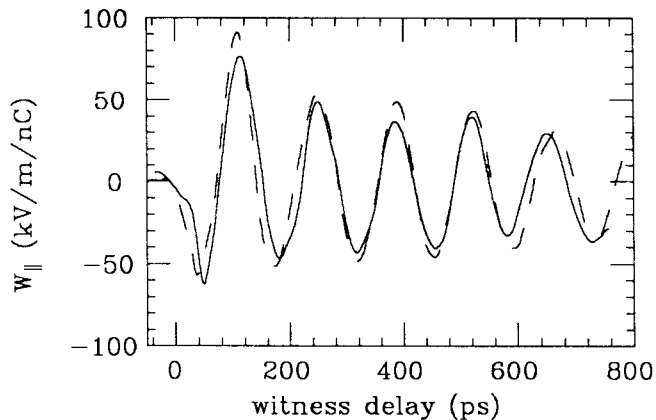


Figure 4: Measured longitudinal wake functions for segmented (dashed) and uniform (solid) outer conductor.

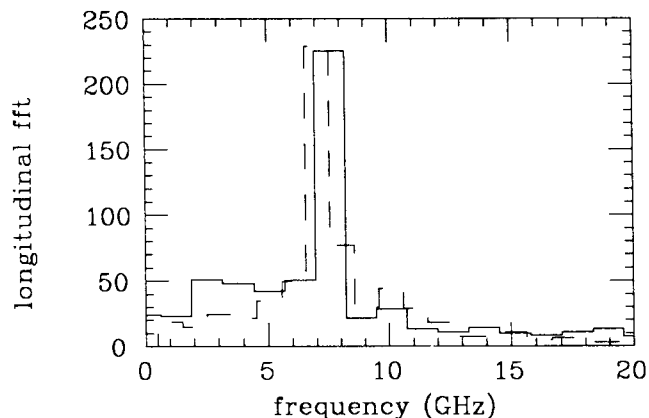


Figure 5: Fourier transforms of longitudinal wake functions shown in Fig. 4.

linearity, and then normalizing to 1 m of axial length, 1 nC of drive charge, and 1 mm of drive bunch radial offset. In Fig. 6 are then shown these normalized *transverse* wake functions for the two Čerenkov wake-field structures with the Fourier transforms shown in Fig. 7. The principle mode in Fig. 7 for the uniform outer conductor is the HEM_{11} , agreeing with the calculated frequency of 6.76 GHz. For the segmented outer conductor, however, the frequency composition is broad band due to the strong attenuation seen in Fig. 6. The attenuation is consistent with the 246 ps e-folding time bench measurement. This demonstration of strong deflection-mode damping thus indicates that bunch-to-bunch beam breakup instabilities can be greatly reduced in Čerenkov wake-field accelerating configurations via use of segmented conducting boundaries followed by rf absorber.

Discussion

We have demonstrated a technique for attenuating deflection-mode wake fields in dielectric slow wave structures using appropriately segmented conductors and rf absorber. The accelerating modes were negligibly affected within resolution of the measurements. A test that remains to be performed is that of voltage standoff between the segmented conductors due to E_{θ} fields which are con-

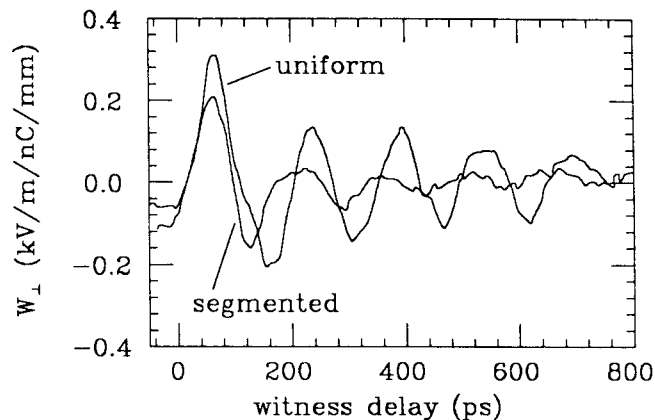


Figure 6: Measured transverse wake functions for segmented and uniform outer conductor.

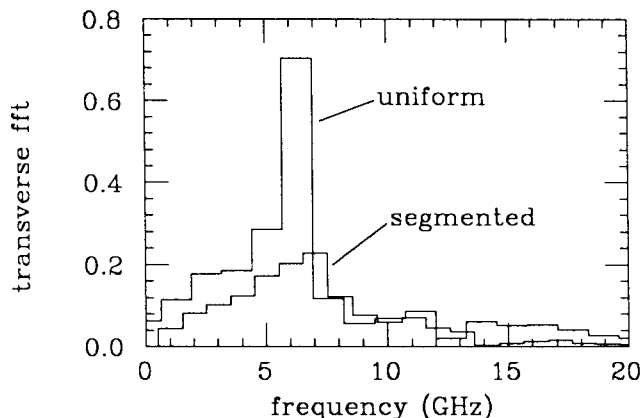


Figure 7: Fourier transforms of transverse wake functions shown in Fig. 6.

tinuous there rather than zero. This test will require smaller waveguide dimensions and the much more intense beam that will be available from the Argonne Wake-field Accelerator linac.[2] The dielectric-lined waveguide should not be susceptible to such rf break down since the conductor is at a large radius, low field density location. The iris-loaded guide will be most vulnerable at the inner edge of the aperture but this can be cured by not segmenting the iris until larger radial positions.

This work supported by the U. S. Department of Energy, Division of High Energy Physics.

References

- [1] R.B. Palmer, DPF Summer Study: Snowmass 1988, Colorado; SLAC-PUB-4542.
- [2] P. Schoessow, E. Chojnacki, W. Gai, C. Ho, R. Konecny, S. Mtingwa, J. Norem, M. Rosing and J. Simpson, Proc. 1990 EPAC Conf., Nice, France (June 11-15, 1990).
- [3] H. Figueroa, W. Gai, R. Konecny, J. Norem, A. Ruggiero, P. Schoessow, and J. Simpson, Phys. Rev. Lett. 60, 2144 (1988).